# Supporting Information

## Integrating Intrinsic Charge Trapping Sites in Insolated MOF Nanoparticles based Dielectric Layer for Effective Photo/Synaptic Transistors

Chaoran Liu[a], Di Sun[a], Ruisi Fan[a], Chengyi Liu[a], Honglin Qiu[a], Qijun Lu[a], Zengqi Xie[a] and Linlin Liu [a, *]

[a]National Key Laboratory of Luminescent Materials and Devices, Institute of Polymer Optoelectronic Materials and Devices, Guangdong Provincial Key Laboratory of Luminescence from Molecular Aggregates,
South China University of Technology,
Guangzhou, 510640, China.
*Corresponding author: Linlin Liu
Email: msliull@scut.edu.cn

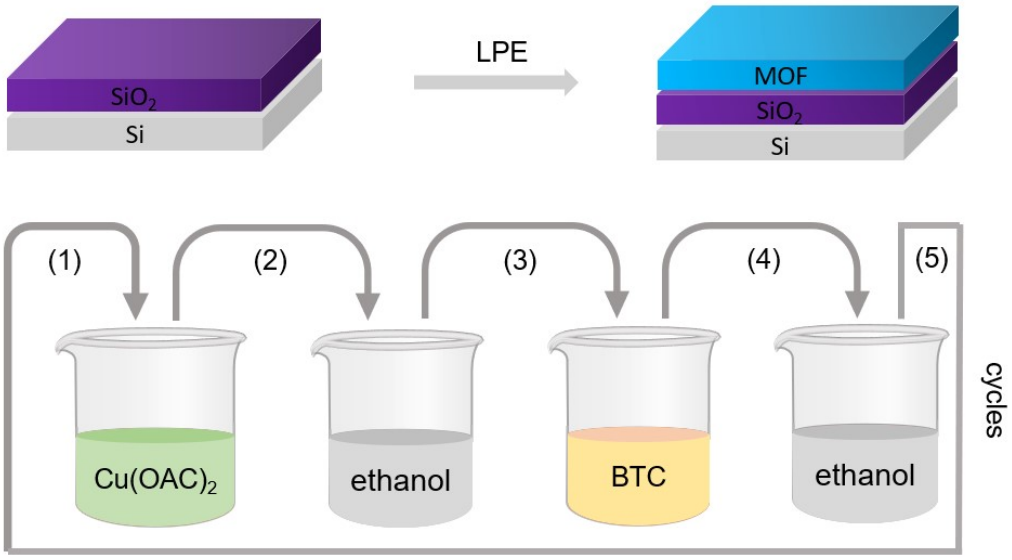


Fig. S1. The liquid phase epitaxy (LPE) layer-by-layer impregnation method

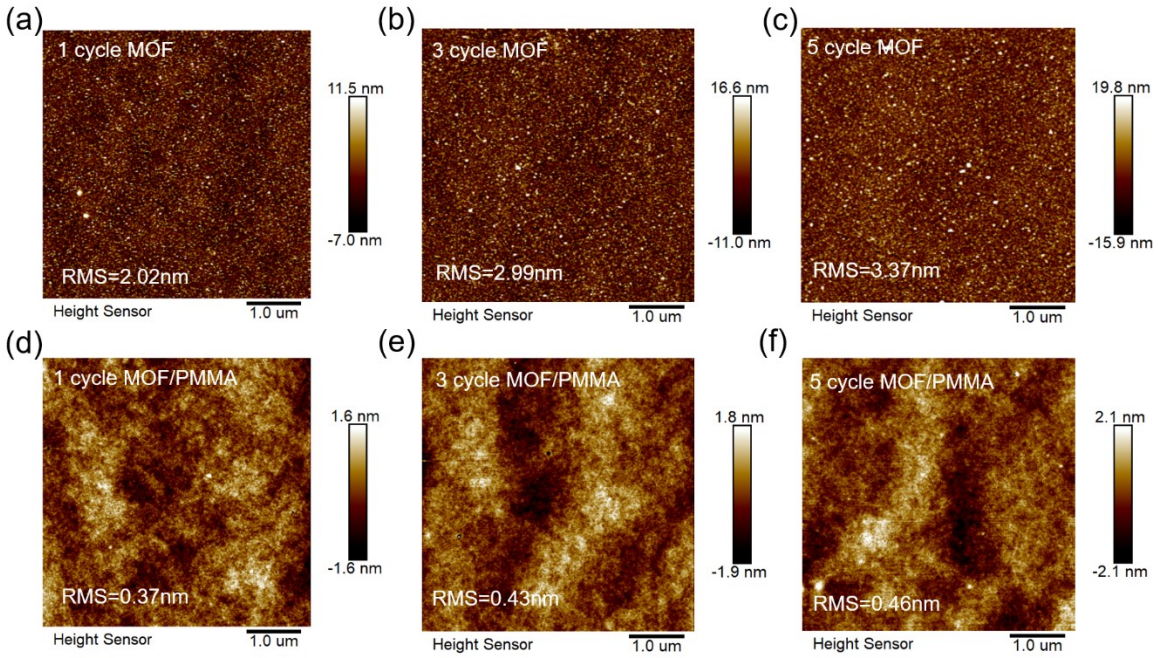


Fig. S2. (a-c) AFM surface images of MOF-NPs films with different LPE dipping cycles, (d-f) spin-coating of PMMA on MOF-NPs films

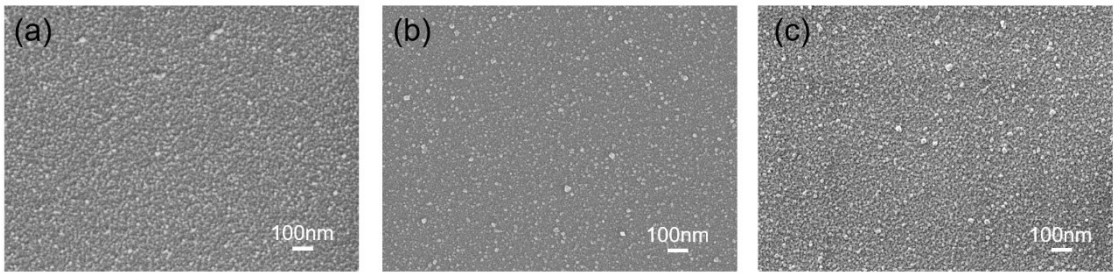


Fig. S3. SEM surface images of MOF-NPs films with different LPE dipping cycles, (a)1 cycle MOF, (b) 3 cycle MOF, (c) 5 cycle MOF

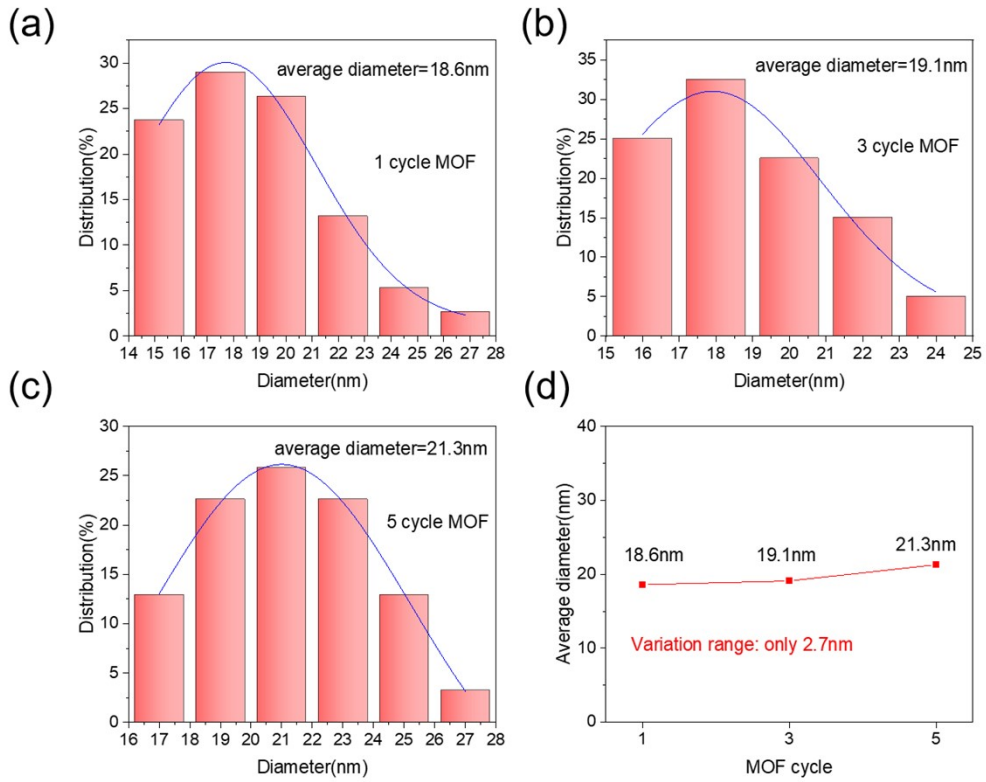


Fig. S4. Size distribution of MOF nanoparticles at different LPE cycles

The size of MOF-NPs can be obtained from the X-ray diffraction spectrum (XRD, Fig. 2c). It can be seen from the XRD spectrum that the 1,3,5 cycle MOF half-height width ($\beta$) values of the diffraction peak at (222) are 0.388, 0.386 and 0.379 respectively, and the corresponding diffraction angles ($\theta$) is 5.922. According to the Scherrer formula:

$$D = \frac{K\lambda}{\beta \cos\theta}$$

where $K$ is the Scherrer constant (0.89), $\lambda$ is the X-ray wavelength (1.54056 Å). The average particle size ($D$) of 1,3,5 cycle MOF-NPs can be calculated in above equation. The calculated $D$ values are 20.31 nm, 20.43 nm and 20.83 nm respectively.

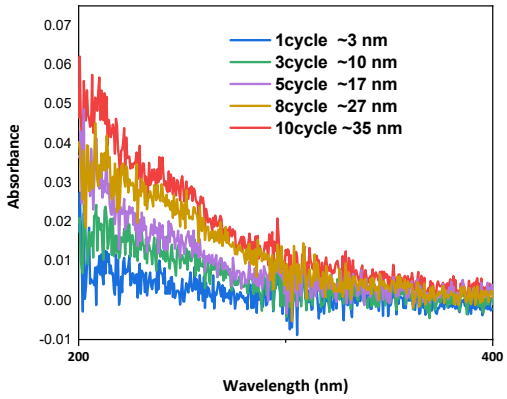


46

47 Fig. S5 Absorption spectra of MOF films with different numbers of deposition cycles and

48 their corresponding thicknesses

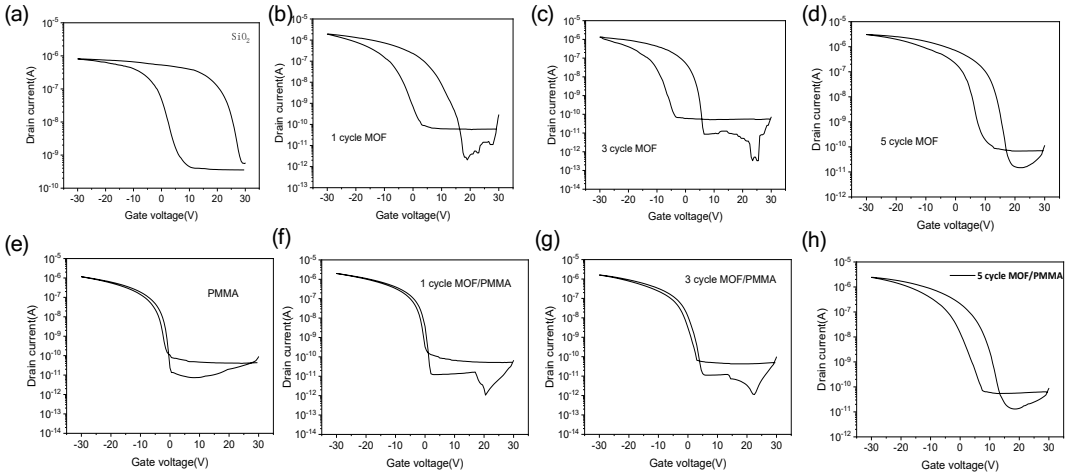


49

50

51 Fig. S6. Forward and reverse transfer curves in dark under transistors with different cycles

52 of MOFs

53

54

55

56

57

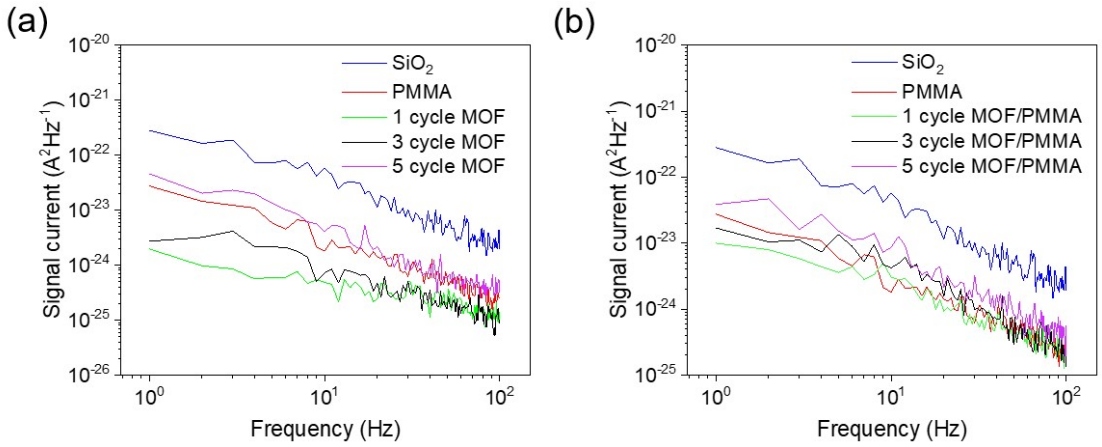


Fig. S7. 1/f noise current curves of different dielectric layer devices, (a) MOF-NPs films devices,(b) MOF-NPs /PMMA films devices

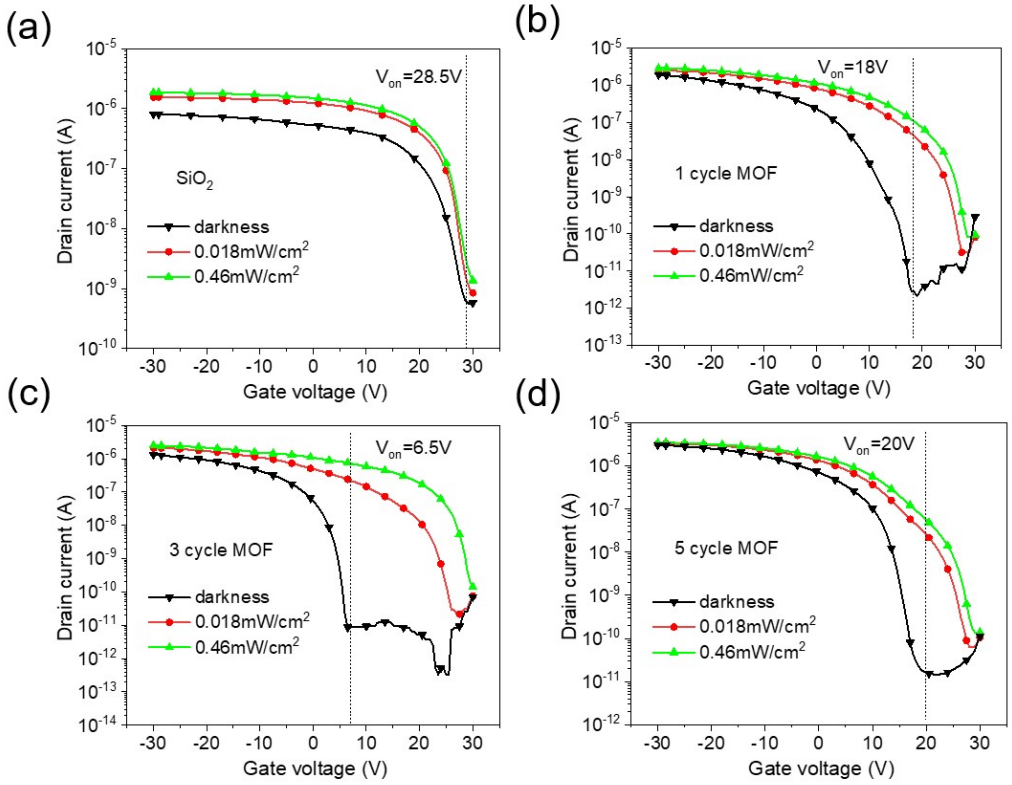


Fig. S8. Transfer characteristics curves of different dielectric layer devices without illumination and in different light intensity illumination of 810 nm, the drain voltage is set to −60 V, (a)$SiO_2$, (b)1 cycle MOF, (c) 3 cycle MOF, (d) 5 cycle MOF

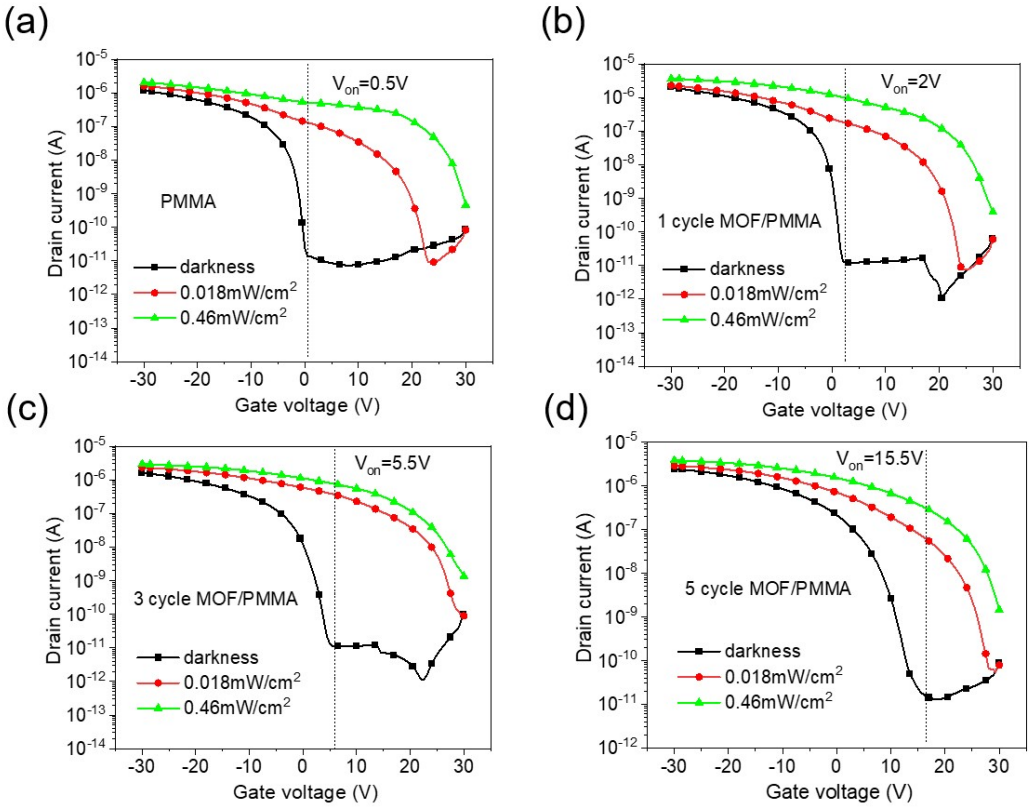


Fig. S9. Transfer characteristics curves of different dielectric layer devices without illumination and in different light intensity illumination of 810 nm, the drain voltage is set to −60 V, (a)PMMA (b)1 cycle MOF/PMMA, (c) 3 cycle MOF/PMMA, (d) 5 cycle MOF/PMMA

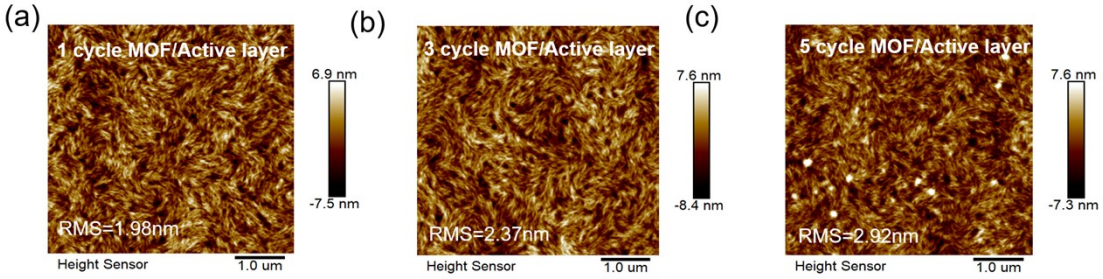


Fig.S10.AFM surface images of MOF/PDPPBTT:$PC_{61}BM$ films with different LPE dipping cycles.

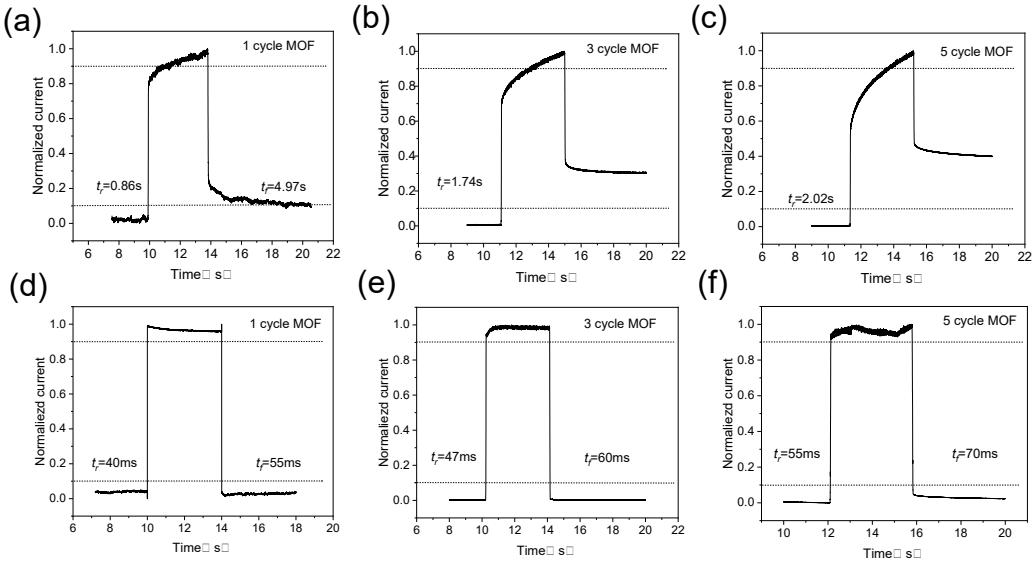


77
78

79 Fig. S11. Time responses of different dielectric layer devices only under light illumination
80 and light co-control method at -60 V drain voltage, (a-c)1,3,5cycle MOF only under light
81 illumination, respectively. (d-f) 1,3,5cycle MOF under light co-control method,

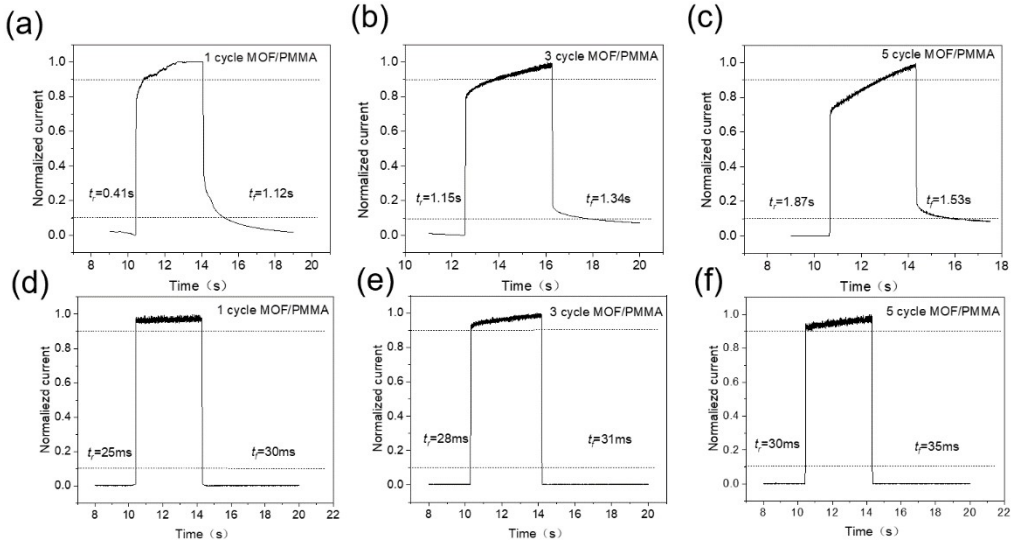


82 respectively.

83

84 Fig. S12. Time responses of different dielectric layer devices only under light illumination
85 and light co-control method at -60 V drain voltage, (a-c)1,3,5cycle MOF/PMMA only
86 under light illumination, respectively. (d-f)1,3,5cycle MOF/PMMA under light co-control
87 method, respectively.

Table.S1 Photodetection performance parameters of devices with different dielectric layers

| dielectric layer | $V_{on}$ [V] | $\Delta V_{on}$ [V] | $I_{light}/I_{dark}$ [$\times 10^3$] | $R$ [$A \cdot W^{-1}$] | $G$ | $D_{shot}$* [$\times 10^{14}$ Jones] | $D_{1/f}$ [$\times 10^{13}$ Jones] | $t_r$ [ms] | $t_f$ [ms] |
|---|---|---|---|---|---|---|---|---|---|
| $SiO_2$ | 28.5 | 1.5 | 0.00278 | 2.1 | 3.1 | 0.23 | 0.032 | 1450 | 45 |
| PMMA | 0.5 | 21.5 | 9.67 | 226.6 | 346.7 | 21.7 | 25.1 | 25 | 37 |
| 1 cycle MOF | 18 | 9.5 | 17.6 | 84.4 | 129 | 17.9 | 13.6 | 40 | 55 |
| 3 cycle MOF | 6.5 | 20 | 27.8 | 417 | 638 | 50.1 | 72.6 | 47 | 60 |
| 5 cycle MOF | 20 | 8 | 1.59 | 44.2 | 67.7 | 3.89 | 6.14 | 55 | 70 |
| 1 cycle MOF/PMMA | 2 | 22.5 | 13.6 | 317.7 | 486.1 | 30.6 | 37.5 | 25 | 30 |
| 3 cycle MOF/PMMA | 5.5 | 24.5 | 32.6 | 650.1 | 994.5 | 67.6 | 72.1 | 28 | 31 |
| 5 cycle MOF/PMMA | 15.5 | 14 | 10.2 | 127.6 | 195.2 | 16.8 | 10.8 | 30 | 35 |

Concrete parameters of OPTs at −60 V drain voltage under 810nm@0.018 mW $cm^{-2}$ illuminations

Table.S2 Materials and performance comparison of different types of phototransistors

| Active layer | R($A\ W^{-1}$) | $D_{shot}$*(Jones) | Ref. |
|---|---|---|---|
| C8-BTBT：$PC_{61}BM$ | $8.6\times10^3$ | $3.4\times10^{14}$ | [S1] |
| ZIF-8 | 70.7 | $2.14\times10^{16}$ | [S2] |
| Sr-MOF | 1300 | $2.90\times10^{15}$ | [S3] |
| In-TCPP | 30.8 | $7.28\times10^{14}$ | [S4] |
| PDVT-8：$PC_{61}BM$ | 750 | $4.5\times10^{15}$ | [S5] |

Table S3 Comparison of the PPF and EPSC of synaptic transistors reported in different literatures and this work

| Sample | PPF(%) | EPSC(nA) | Data source |
|---|---|---|---|
| IDTBT | 72.8 | 159.46 | [S6] |
| DPP-DTT:N2200 | 140 | 8 | [S7] |
| DPPDTT/SEBS | 132 | 9.5 | [S8] |
| Rubrene | 1.3 | 2 | [S9] |
| $Nb_3Cl_8$ | 4 | 39 | [S10] |
| AZO | 180 | 20 | [S11] |
| In-Zn-O | 400 | 1000 | [S12] |
| 3 cycle MOF | 142 | 588 | This work |

Table S4 Comparison of the $E_{spike}$ of light-controlled synapse-related performance synaptic transistors reported in different literatures and this work

| Sample | $E_{spike}$ | Data source |
|---|---|---|
| Pyrene/Phenanthro | 560 pJ | [S13] |
| Mxene:PVA | 120 mJ | [S14] |
| P3HT/ITIC | 39.6pJ | [S15] |
| ZnO/Al2O3 | 30 pJ | [S16] |
| Al2O3 | 1uJ | [S17] |
| 3 cycle MOF | 100nJ | This work |

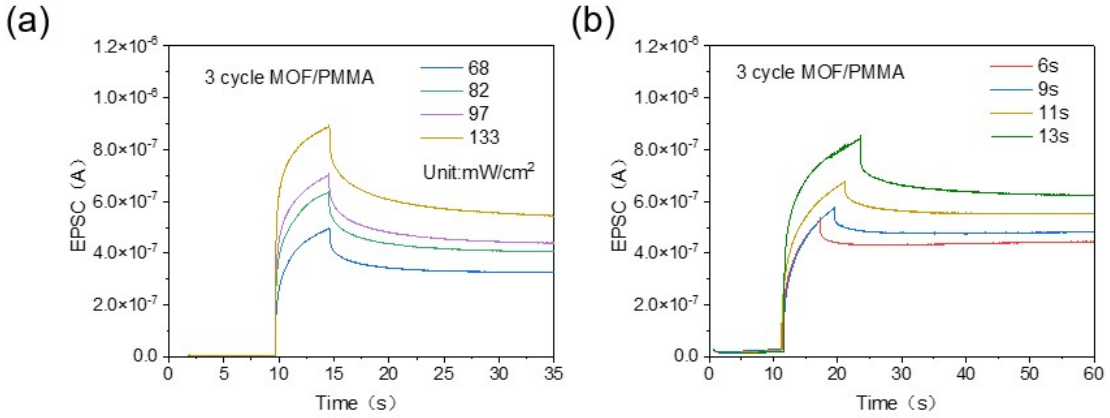


112

113 Fig. S13. Transition of STM to LTM behavior by (a)pulse intensity and (b)pulse width(68
114 mW/cm$^2$, 810 nm)

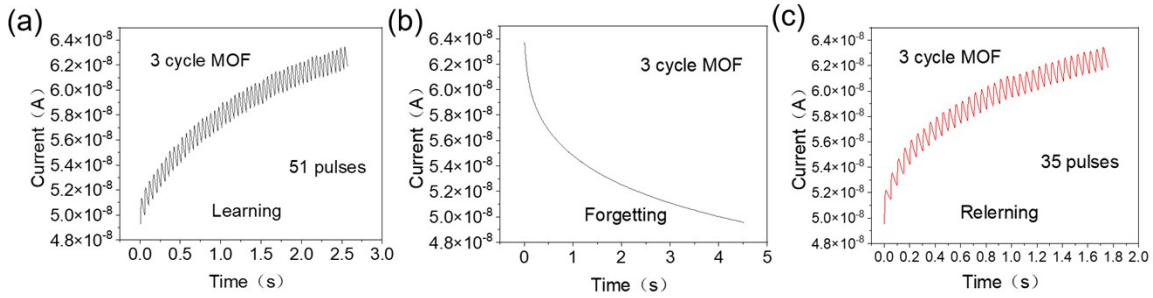


115

116 Fig.S14. "Learning-experience" behavior of the device, including (a)learning,
117 (b)forgetting, and (c)relearning processes.

118

119

120 References


121 S1. Y.H. Gao, Y. Yi, X.W. Wang, et al., *Adv. Mater.*, **2019**, 31, 1900763.

122 S2. T. Guo, C. Ling, X. Li, et al., *J. Mater. Chem. C*, **2019**, 7, 5172.

123 S3. K. P. Bera, Y. G. Lee, M. Usman, et al., *ACS Appl. Electron. Mater.*, **2022**, 4, 2337.

124 S4. Y. B. Tian, N. Vankova, P. Weidler, et al., *Adv. Sci*., **2021**, 8, 2100548.

125 S5. Y. Zhang, Y.B. Yuan, J.S. Huang, *Adv. Mater.,* **2017**, 29, 1603969.

126 S6. H. Yu, J. Sun, X. Zhao, et al., *J. Mater. Sci. Technol.*, **2026**, 249, 12.

127 S7. Y. Ran, W. Lu, X. Wang, et al., *Mater. Horiz.*, **2023**, 10, 4438.

128 S8. D. Hao, T. Chen, P. Guo, et al., *Adv. Compos. Hybrid Mater.*, 2023, 6, 129.

S9. K. Chen, Q. Dai, Y. Tian, et al., *Adv. Funct. Mater.*, **2025**, 2508673.

S10. N. Zhang, Z. Zhang, R. Feng, et al., *ACS Nano*, **2025**, 19, 24109.

S11. N. Lee, P. Pujar and S. Hong, *Biomimetics*, **2024**, 9, 547.

S12. J. Wang, Y. Chen, L.-A. Kong, et al., *Appl. Phys. Lett.*, **2018**, 113.

S13. Y. Ren, C.-L. Chang, L.-Y. Ting, et al., *Adv. Intell. Syst.*, **2019**, 1, 1900008.

S14. X. Zhang, S. Wu, R. Yu, et al., *Matter*, **2022**, 5, 3023.

S15. R. Fan, J. Yu, Z. Xie, et al., *ACS Appl. Mater. Interfaces*, **2025**, 17, 18701.

S16. G. Zhang, Z. Zeng, Y. Yan, et al., *Adv. Funct. Mater.*, **2026**, e31113.

S17. H. Du, F. Wang, Z. Li, et al., *J. Phys. Chem. Lett*., **2025,** 16, 2722.